Supporting information

A green strategy for selective recovery of lithium and synthesis of $CoFe_2O_4$ catalyst for CO oxidation from spent lithium-ion batteries

Minyu He, Weizao Liu*, Meijie Gao, Pengyang Zhang, Xi Jin, Hongli Wu*, Qingcai Liu

College of Materials Science and Engineering, Chongqing University, Chongqing 400044, China

*Corresponding author: liuwz@cqu.edu.cn (W. Liu), hongliwu@cqu.edu.cn (H. Wu)

Supporting Information Content

9 pages (including the cover page)

1 Text: Material and methods

4 Tables

6 Figures

Text 1: Material and methods

Spent LCO batteries were purchased from a waste treatment plant located in Sichuan Province, China. The waste copperas was supplied by LB Sichuan Titanium Industry Co., Ltd. The initial step in the experimental protocol involved the discharge of the spent lithium-ion batteries in a 5wt% NaCl solution for 48 hours to eliminate any residual electricity. Subsequently, the discharged batteries were manually dismantled into their constituent parts, including cathode plates, anode plates, shells, and separators. To recover the cathode powder and Al foil, the active cathode plates were subjected to heat treatment in a muffle furnace at 450°C for 240 minutes to eliminate the organic binder. The composition of the obtained cathode powder was determined by X-ray fluorescence spectrometer (XRF) and inductively coupled plasma optical emission spectrometry (ICP-OES). The chemical compositions of the active cathode powder and copperas are provided in Table. After pretreatment, the active cathode powder contained 54.37% Co and 6.67% Li, respectively. The active cathode powder contained 34.08% Fe and 18.91% S, respectively.

Table S1. Chemical composition of the cathode powder of spent LCO battery (wt%)

Composition	Co	Li	Al	Ni	Mn	Fe	S	Ti	Mg
Cathode powder	54.37	6.67	0.08	0.06	0.01	-	-	-	-
Copperas	-	-	0.02	-	-	34.08	18.91	0.86	1.2

Preparation of CO catalyst and analysis methods

Leach residue and $Fe(NO_3)_3 \cdot 9H_2O$ (Calculated to be 30% of total catalyst mass for cobalt oxides) were mixed with 20mL and 50mL of N,N-dimethylformamide (DMF, AR, CHRON

CHEMICALS), respectively. The uniformly dispersed cobalt-iron suspension and homogeneous $Fe(NO_3)_3$ solution were obtained by 30 min of sonication. The $Fe(NO_3)_3$ solution was then added dropwise to the cobalt-iron suspension under stirring for 30 min. Subsequently, $NH_3 \cdot H_2O$ was also added dropwise to the above mixed suspension and stirred for 60 min until pH=9. To remove the remaining nitrate and organic solvent, the resulting precipitate was washed several times with ethanol (by centrifugation or extraction) and dried at 80°C for 12 h. Afterwards, the dried powder was annealed at 400°C (2°C/min) for 2 h and cooled to ambient temperature to obtain the CO catalyst.

Qualitative analysis of solid samples was investigated utilizing an XRD (Bruker D8 Advance X-ray Diffractometer) equipped with 1.5406 Å Cu Kα radiation. The active cathode powder composition was characterized via X-ray fluorescence spectrometry (XRF-180, Shimadzu, Japan). Field emission scanning electron microscopy (SEM, SU-1500, Hitachi, Japan) was used to observe the microscopic morphology of both the cathode powder and roasted samples. X-ray photoelectron spectroscopy (XPS, Thermo escalab 250Xi) was used to characterize the chemical state of surface element of sample. In the recycling process, quantitative analysis of metal elements was measured using inductively coupled plasma-atomic emission spectrometry (ICP-AES, IRIS Advantage 1000, THERMO, U.S.) after complete dissolution of the samples with a mixture of 2mol/L H_2SO_4 and 30 wt % H_2O_2 in a 1:1 (v/v) ratio. Thermodynamic parameters such as the standard Gibbs enthalpy changes (ΔH^{Θ}), free energy change (ΔG^{Θ}), and equilibrium composition of the reaction system were calculated using HSC Chemistry 9.0. Finally, the concentrations of emitted SO_2 were measured via a flue gas analyzer (Thermo Scientific, Antaris IGS). CO-TPD, the samples were pretreated by a flue

gas analyzer(Thermo Scientific, Antaris IGS). The pretreated sample was cooled down to room tem-perature under a helium atmosphere and then CO were injected for 0.5h. After that, the sample was purged with N_2 for 1h and heated to 600°C with a ramping rate of 10°C/min. The structural and electronic structural properties of LCO, $LiFeO_2$, FeSO4 and $CoFe_2O_4$ by the calculating Partial Density of States (PDOS), DOS package of the Material Studio (MS) software, and the bond length bond energy was calculated using DFT. Raman spectra of the catalysts were obtained by Raman spectroscopy (France Horiba, HREvolution) with a laser wavelength of 532 nm. UV−visible absorption spectroscopy was performed on a spectrometer (Japan, Shimadzu UV-3600i Plus) equipped with an integrating sphere. Hydrogen temperature-programmed reduction (H_2-TPR) was tested in a continuous-flow device equipped with a TCD detector. Using CO as the probe molecule, the evolution of the adsorbed species on the catalyst surface during the CO adsorption, desorption and oxidation reactions was studied with a diffuse reflectance infrared spectrometer (DRIFTS, Thermo iS50).

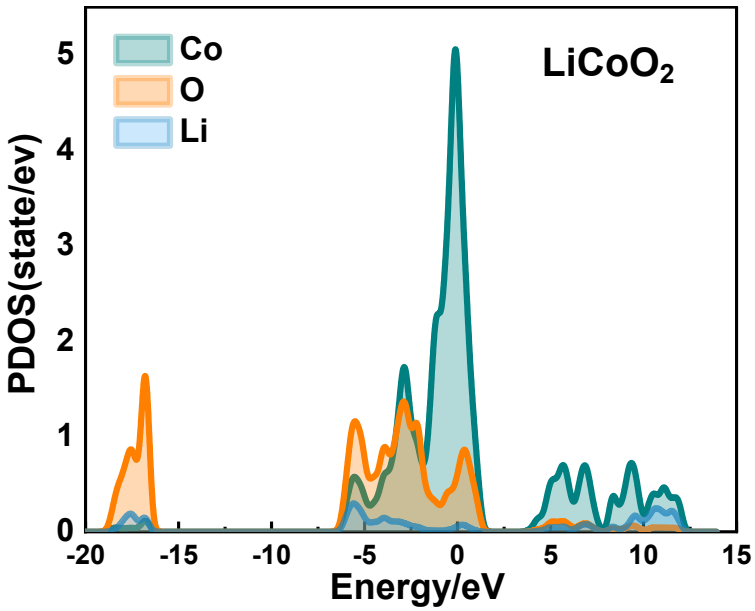

Figure S1. Partial density of states of $LiCoO_2$

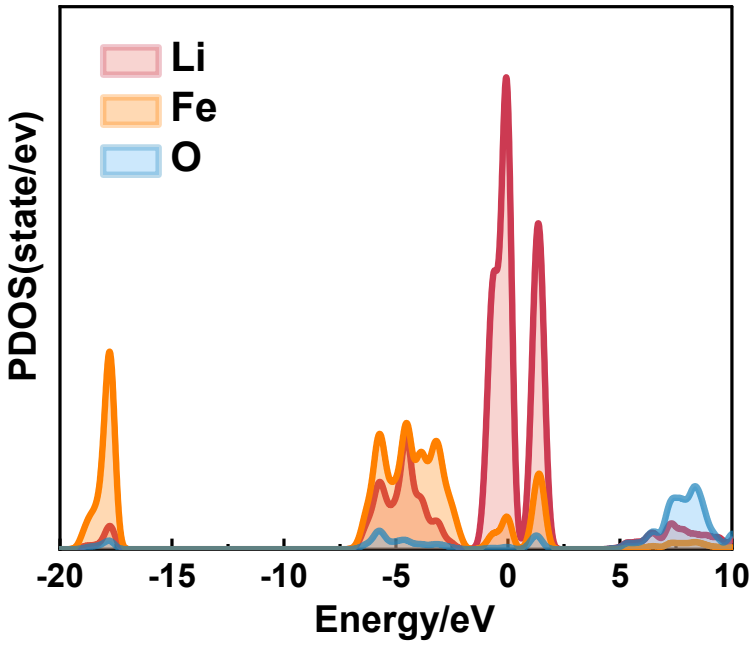

Figure S2. Partial density of states of $LiFeO_2$

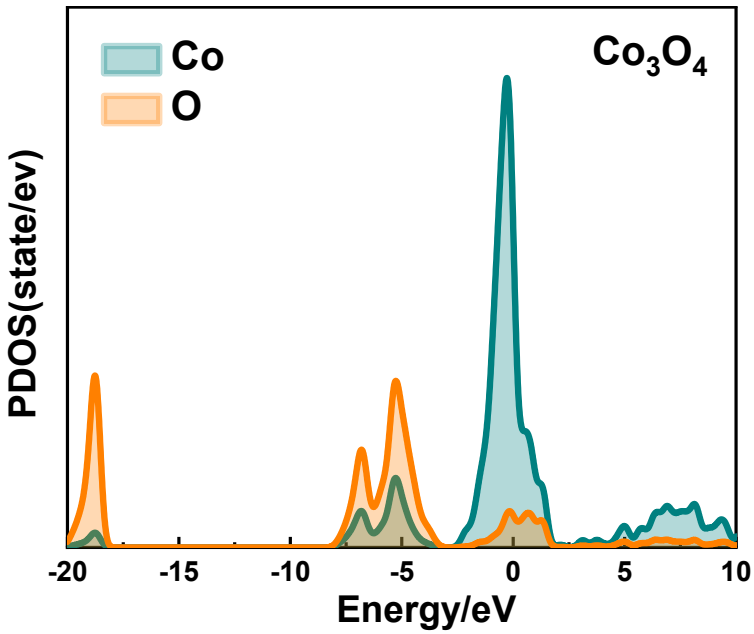

Figure S3. Partial density of states of Co_3O_4

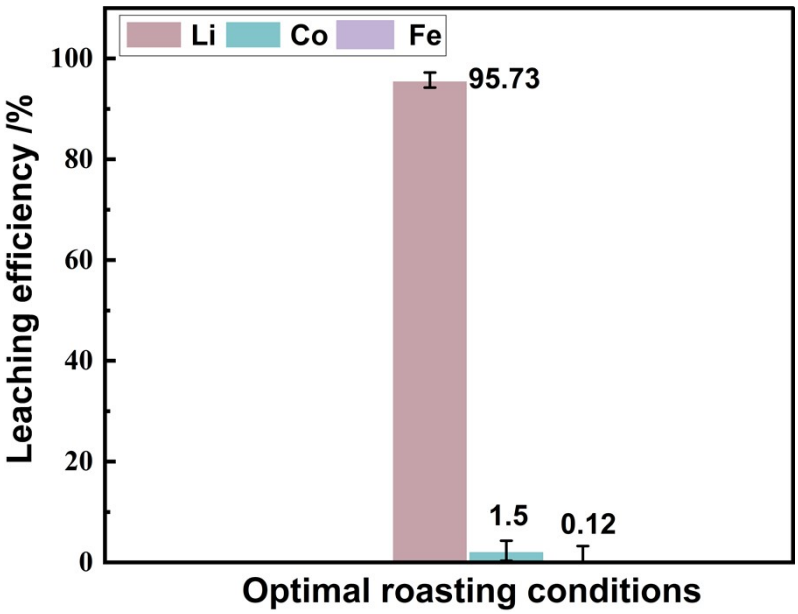

Figure S4. The leaching efficiency of lithium, cobalt and iron under optimal roasting conditions.

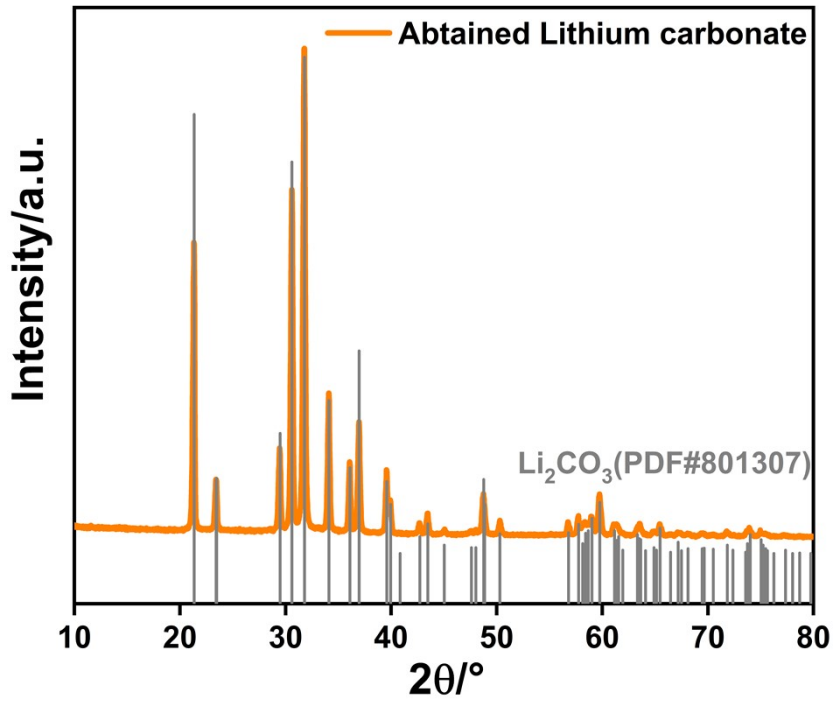

Figure S5. XRD pattern of the obtained lithium carbonate.

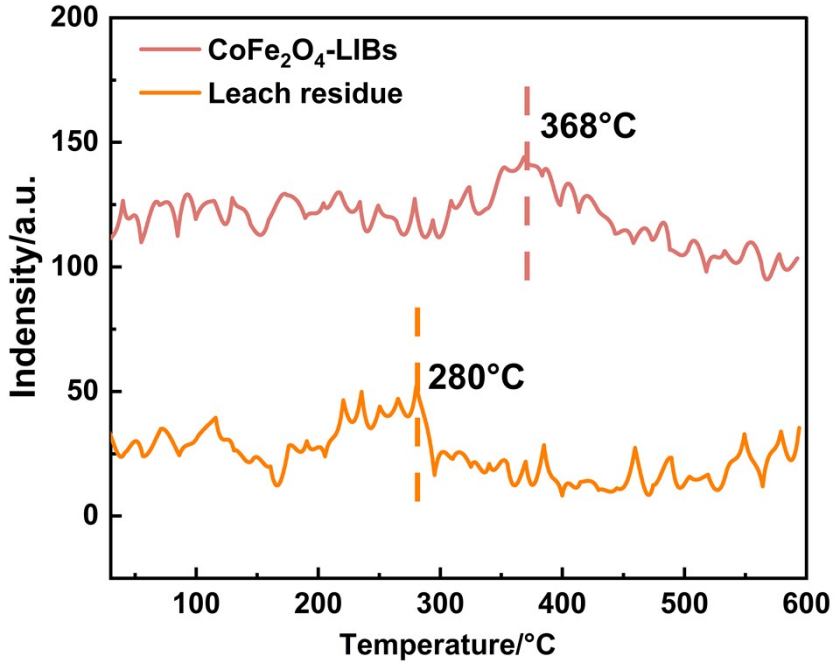

Figure S6. CO -TPD profiles of the leach residue and $CoFe_2O_4$-LIBs samples.

Table S2. Chemical compositions of the obtained Li_2CO_3 product (wt %)

Li_2CO_3	Co_3O_4	Al_2O_3	Na_2O
99.69	0.074	0.069	0.089

Table S3. Performance comparison between LIBs-derived $CoFe_2O_4$ and other widely-used catalysts for CO oxidation

Catalyst	**Operating parameters**	**CO catalytic oxidation efficiency**	**Reference**
4.5%Ag/$Ce_{0.67}Zr_{0.33}O_2$	The 60 mg catalyst in presence of 5% O_2 in air at a total flow velocity 5000 h^{-1} in a temperature range of 150–500 °C	**T_{100} = 282 °C**	Lee et al.[1,2]
2%Ru+CeO_2	The catalyst in presence of 10% O_2 and 4000ppm CO in air at a total flow velocity 600000 h^{-1} in a temperature range of 0–300 °C	**T_{100} = 180 °C**	Satsuma et al.[3]

Nanosized Fe_2O_3	The catalyst weight 0.3,1,2, and 3g in presence of 24% CO, 38% O_2, 38% N_2 with temp. range 200-500°C	**T_i= 200°C, T_{50} = 320°C, T_{100}=500°C**	Khedr et al.[4]
$NiFe_2O_4$	The 100 mg catalyst in presence of 2 ppm CO, 5 ppm N_2 balanced air at temp. 100 °C for 2h	**T= 125°C, T_{50} =210°C, T_{100} =280°C**	Maity et al.[5]
Ni-Cu-CrO	The 100 mg catalyst in presence of 1% CO in air at a total flow velocity 36,000 h^{-1} in a temperature range of 100–500 °C	**T_i=105 °C, T_{50}= 350 °C, T_{100}=500 °C**	Xanthopoulou et al.[6]
$CuO-TiO_2$	The 2 gm catalyst with a reaction gases compositions of 5 vol% CO balanced with air. The total gases flow was 0.5 l/min and GHSV was 30,000 h^{-1}	**T_i=50 °C, T_{50}=140 °C, T_{100}= 200 °C**	Dehestaniathar et al.[7]
Fe_2O_3-NiO	The 100 mg catalyst with 1.5 vol% CO_2 vol% O_2 balanced with N_2 at flow velocity of 100 ml/min	**T= 360°C, T_{50} =545°C, T_{100} =830°C**	Li et al.[8]
$CoFe_2O_4$-LIBs	The 0.3g catalyst in presence of a mixture of 1vol% CO (1000 ppm), 5vol% O_2 in air at a total flow velocity 45000 h^{-1} in a temperature range of 150–500 °C	**T_i=100 °C, T_{50}=220 °C, T_{100}= 350 °C**	This study

Note: T_i represents the initial temperature at which CO is oxidized. T_{50} represents the temperature at which the CO conversion rate is 50%. T_{100} represents the temperature at which the CO conversion rate is 100%

Table S4. The surface area and nitrogen adsorption-desorption isotherms and corresponding pore volume distributions of leaching residue and $CoFe_2O_4$-LIBs sample.

Samples	Surface area(m^2/g)	Pore volume(cm^3/g)	Pore diameter(nm)
Leaching residue	4.994	0.007	3.197

$CoFe_2O_4$-LIBs	32.527	0.064	6.521

Reference:

1. C. Lee, Y. Jeon, T. Kim, A. Tou, J.-I. Park, H. Einaga and Y.-G. Shul, *Fuel*, 2018, **212**, 395-404.

2. J. Lee, Y. Ryou, J. Kim, X. Chan, T. J. Kim and D. H. Kim, *The Journal of Physical Chemistry C*, 2018, **122**, 4972-4983.

3. A. Satsuma, M. Yanagihara, J. Ohyama and K. Shimizu, *Catal. Today*, 2013, **201**, 62-67.

4. M. H. Khedr, K. S. A. Halim, M. I. Nasr and A. M. El-Mansy, *Materials Science and Engineering: A*, 2006, **430**, 40-45.

5. A. Maity, A. Ghosh and S. B. Majumder, *Sensors and Actuators B: Chemical*, 2016, **225**, 128-140.

6. G. Xanthopoulou , G. Vekinis, *Appl Catal B-Environ* , 1998, **19**, 37-44.

7. S. Dehestaniathar, M. Khajelakzay, M. Ramezani-Farani and H. Ijadpanah-Saravi, *J. Taiwan Inst. Chem. Eng.*, 2016, **58**, 252-258.

8. B. Li, Y.-g. Wei and H. Wang, *Transactions of Nonferrous Metals Society of China*, 2014, **24**, 3710-3715.